Electronic Supplementary Material (ESI) for Nanoscale.

Supporting information:

Using Rotation to Organize Cellulose Nanocrystals Inside a Fiber

Arash Momeni [a], Wadood Y. Hamad [b], Mark J. MacLachlan* [a,c,d,e]

[a] Department of Chemistry, University of British Columbia, 2036 Main Mall, Vancouver, British Columbia V6T 1Z1, Canada
[b] Transformation and Interfaces Group, Bioproducts Innovation Centre of Excellence, FPInnovations, 2665 East Mall, Vancouver, British Columbia V6T 1Z4, Canada
[c] Stewart Blusson Quantum Matter Institute, 2355 East Mall, Vancouver, British Columbia, V6T 1Z4, Canada
[d] WPI Nano Life Science Institute, Kanazawa University, Kanazawa, 920-1192, Japan
[e] UBC BioProducts Institute, 2385 East Mall, Vancouver, British Columbia, V6T 1Z4, Canada

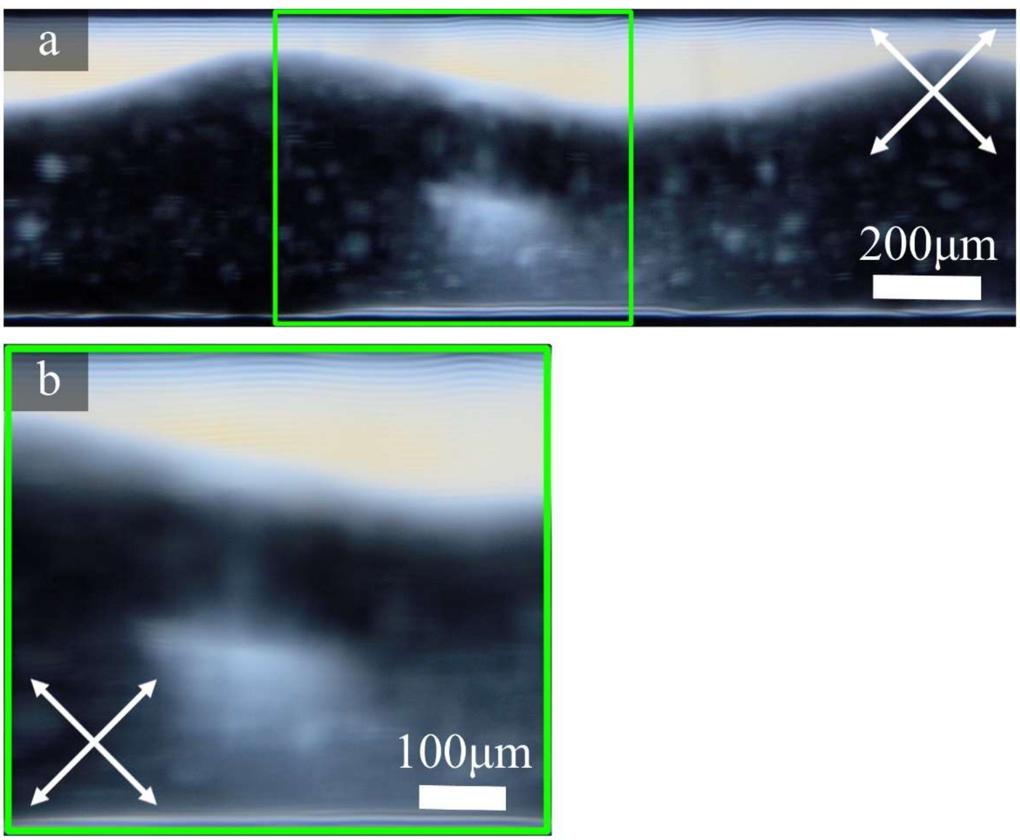

Figure S1. Polarized optical microscopy (POM) images of 4.5 wt.% CNC suspension rotated at 0.16 s^{-1} (1.5 rpm) (low rotation regime); a) low magnification, b) high magnification of green box of image (a). Note the peaks and troughs of the anisotropic domain at longitudinal direction. Note the birefringent periodic fingerprint lines of the anisotropic region, an indicator of chiral nematic structure.

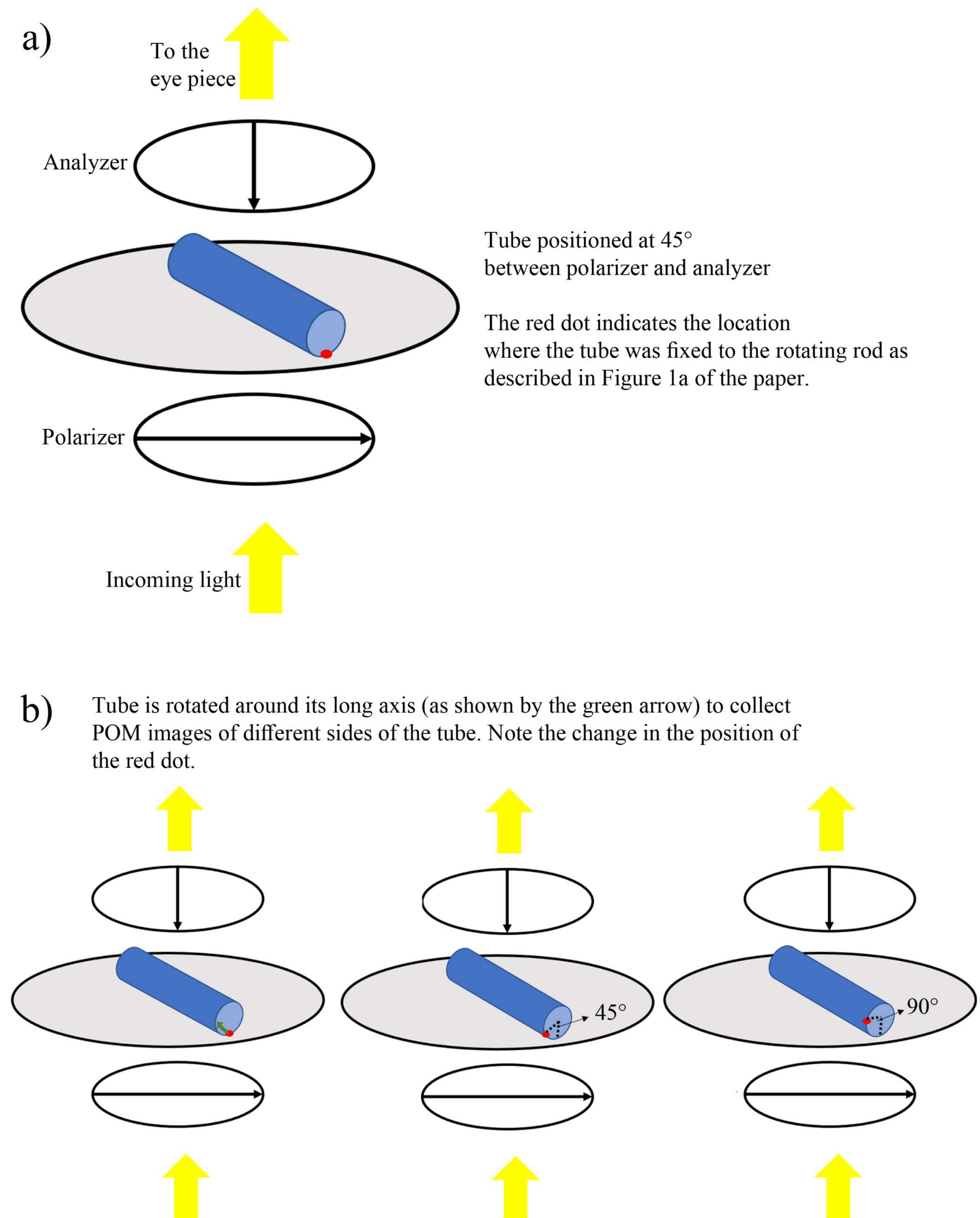

Figure S2. Schematic of POM techniques; a) POM imaging of the tubes showing the orientation of the tube, b) POM imaging of the tube at different rotation angles of the tube to collect images of different sides of the tube. Using this technique, it was possible to locate the position of the anisotropic domain.

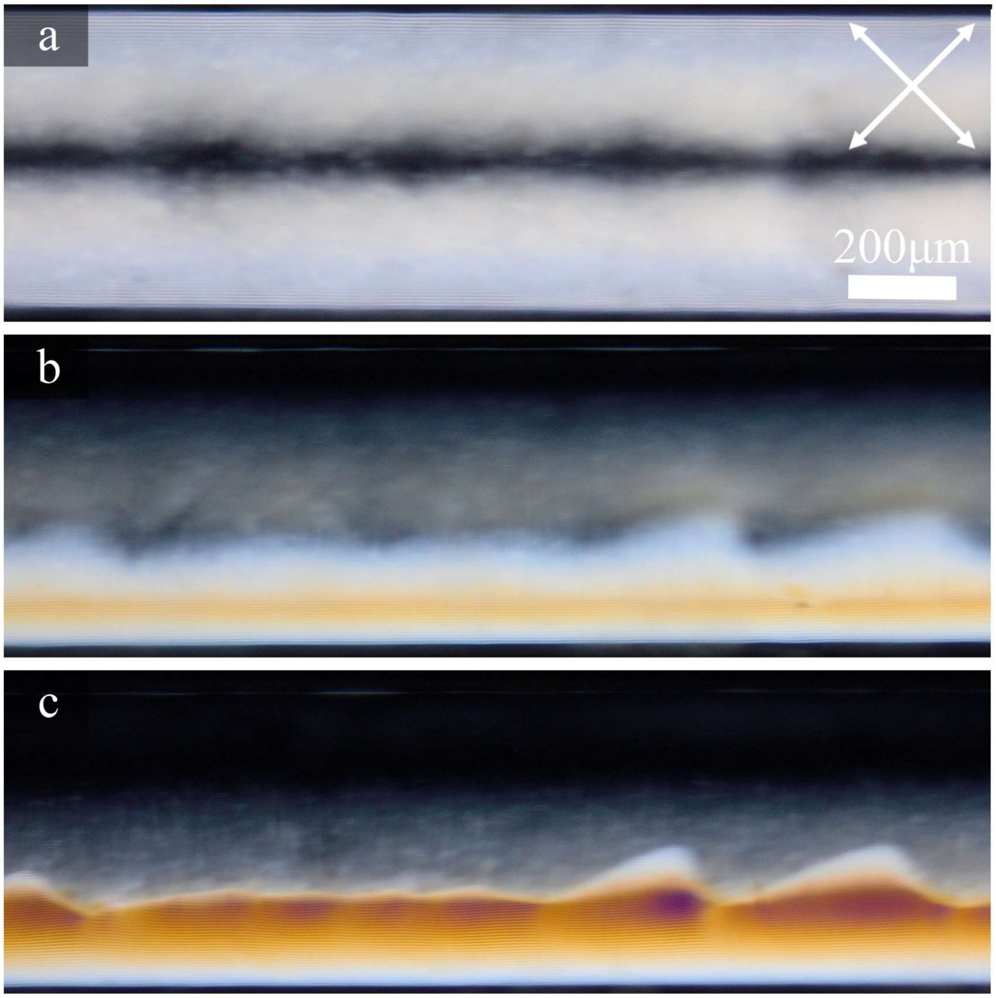

Figure S3. POM images of 5 wt.% CNC at 0 s^{-1} (in absence of rotation). The same position of the tube is imaged at different rotation angles of 0° (a), 45° (b), and 90° (c) as described in Figure S2-b. The 0° image is similar to that provided in Figure 3 of the manuscript. These rotation POM images confirm that the anisotropic domain is at the bottom of the tube.

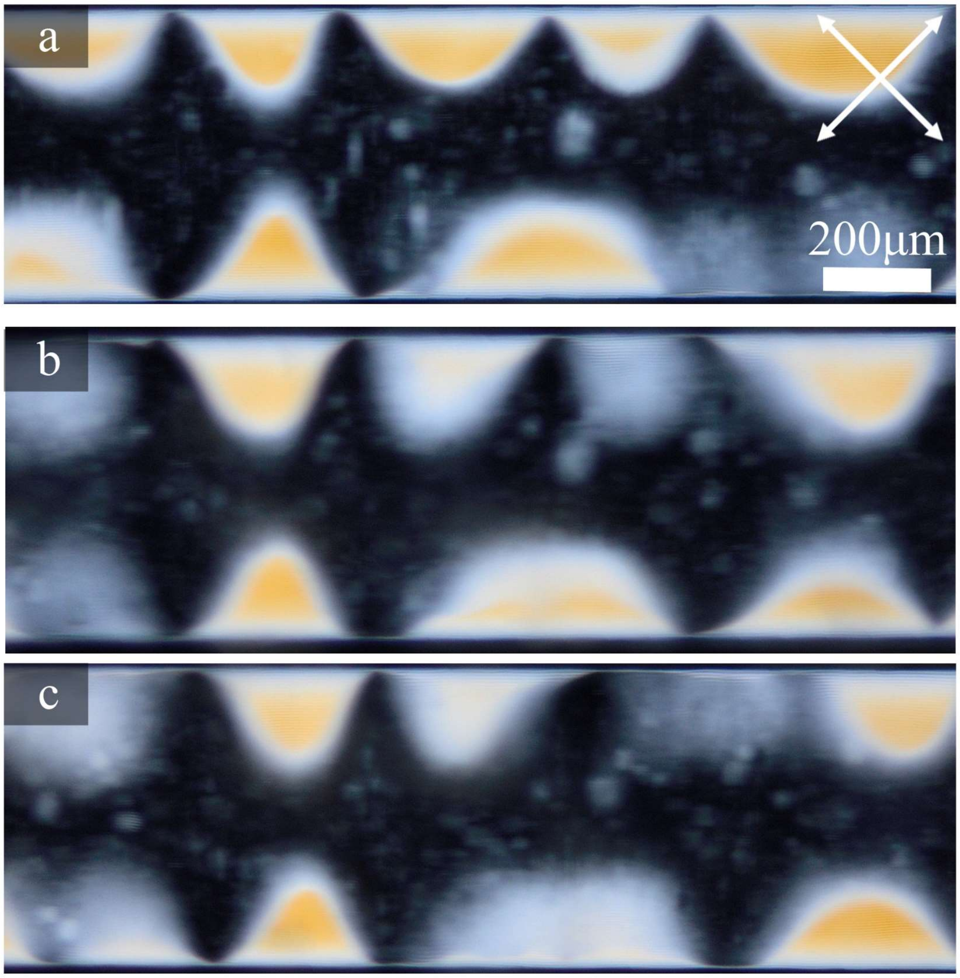

Figure S4. POM images of 5 wt.% CNC rotated at 2.6 s^{-1}. The same position of the tube is imaged at different rotation angles of 0° (a), 45° (b), and 90° (c) as described in Figure S2-b. The 0° image is similar to that provided in Figure 3 of the manuscript. These rotation POM images confirm that the anisotropic domain is concentrated at sides of the tube at some locations and at other locations they are at the top and bottom.

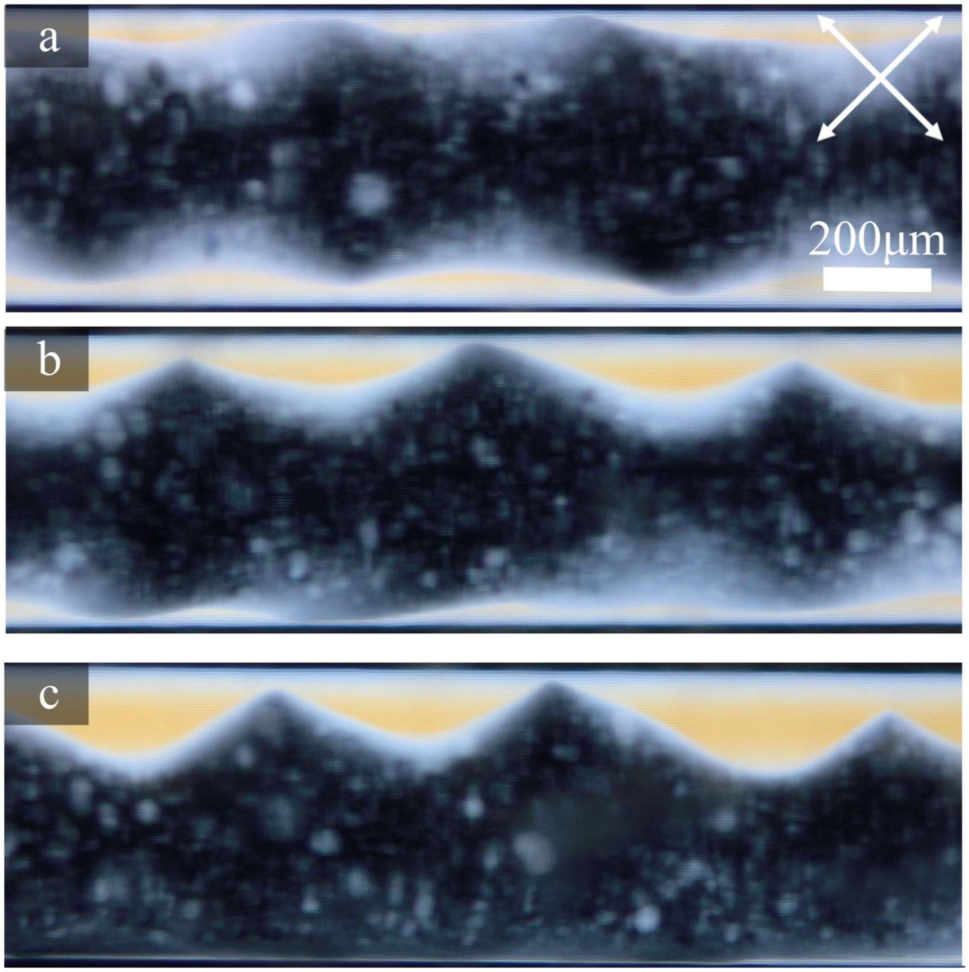

Figure S5. POM images of 5 wt.% CNC rotated at 6.3 s^{-1}. The same position of the tube is imaged at different rotation angles of 0° (a), 45° (b), and 90° (c) as described in Figure S2-b. The 0° image is similar to that provided in Figure 3 of the manuscript. These rotation POM images confirm that the anisotropic domain is concentrated at the top of tube, forming a wavy pattern at the top.

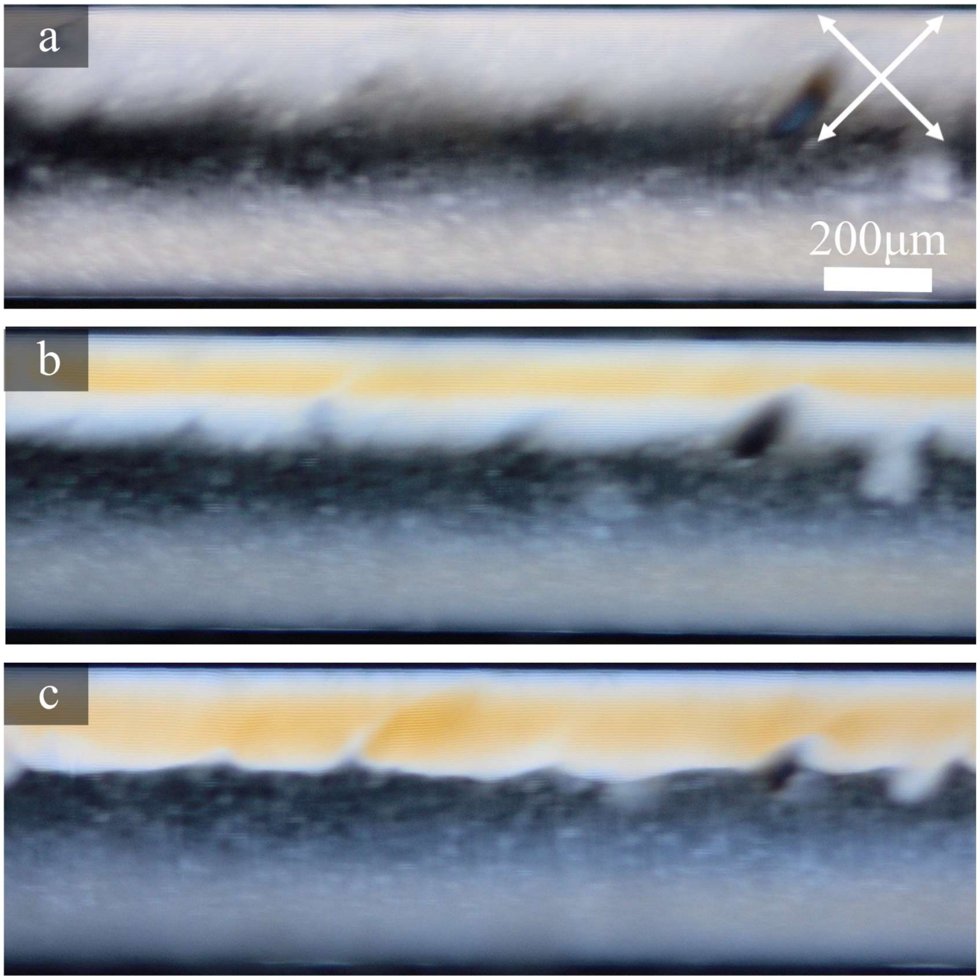

Figure S6. POM images of 5 wt.% CNC rotated at 52 s^{-1}. The same position of the tube is imaged at different rotation angles of 0° (a), 45° (b), and 90° (c) as described in Figure S2-b. The 0° image is similar to that provided in Figure 3 of the manuscript. These rotation POM images confirm that the anisotropic domain is concentrated at the top of the tube, forming a relatively smooth pattern at the top.

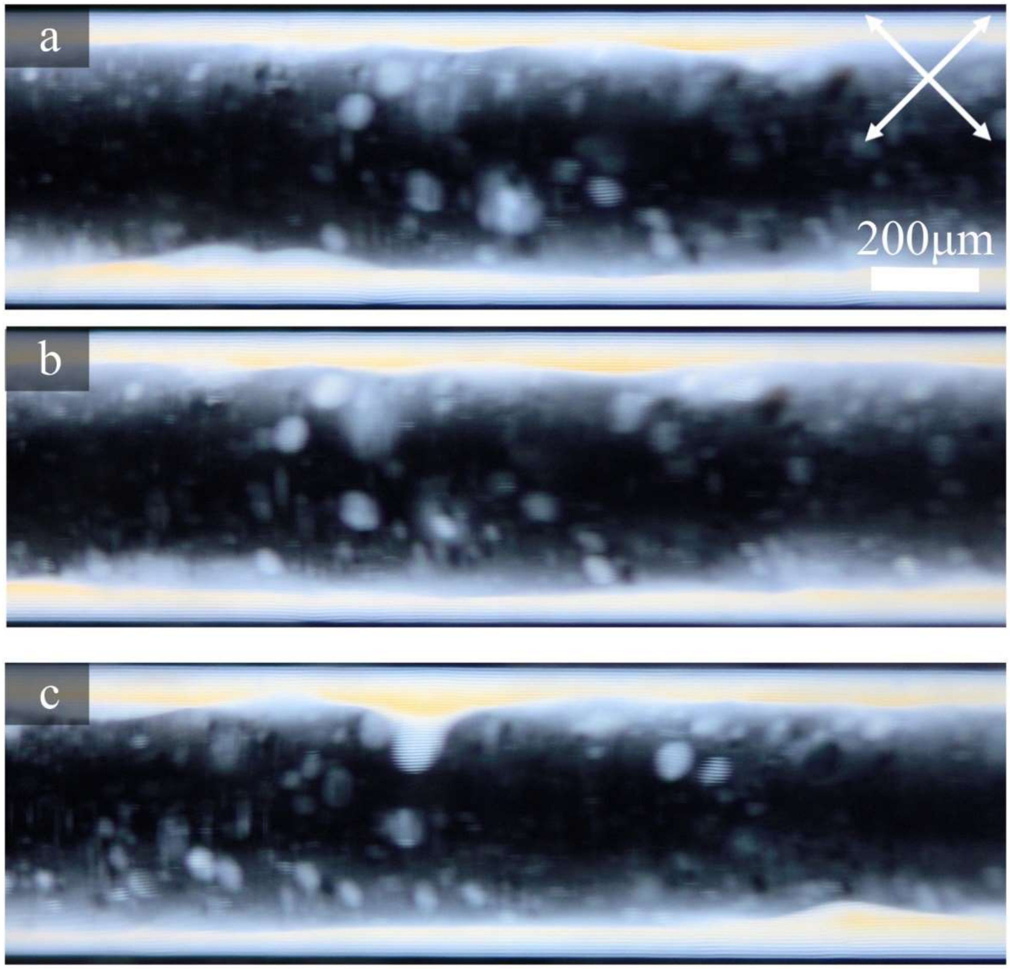

Figure S7. POM images of 5 wt.% CNC rotated at 6.3 s^{-1} while tilted at α=45°. The same position of the tube is imaged at different rotation angles of 0° (a), 45° (b), and 90° (c) as described in Figure S2-b. The 0° image is similar to that provided in Figure 4 of the manuscript. These rotation POM images confirm that the anisotropic domain is uniformly distributed around the circumference of the tube, forming the core-shell structure.

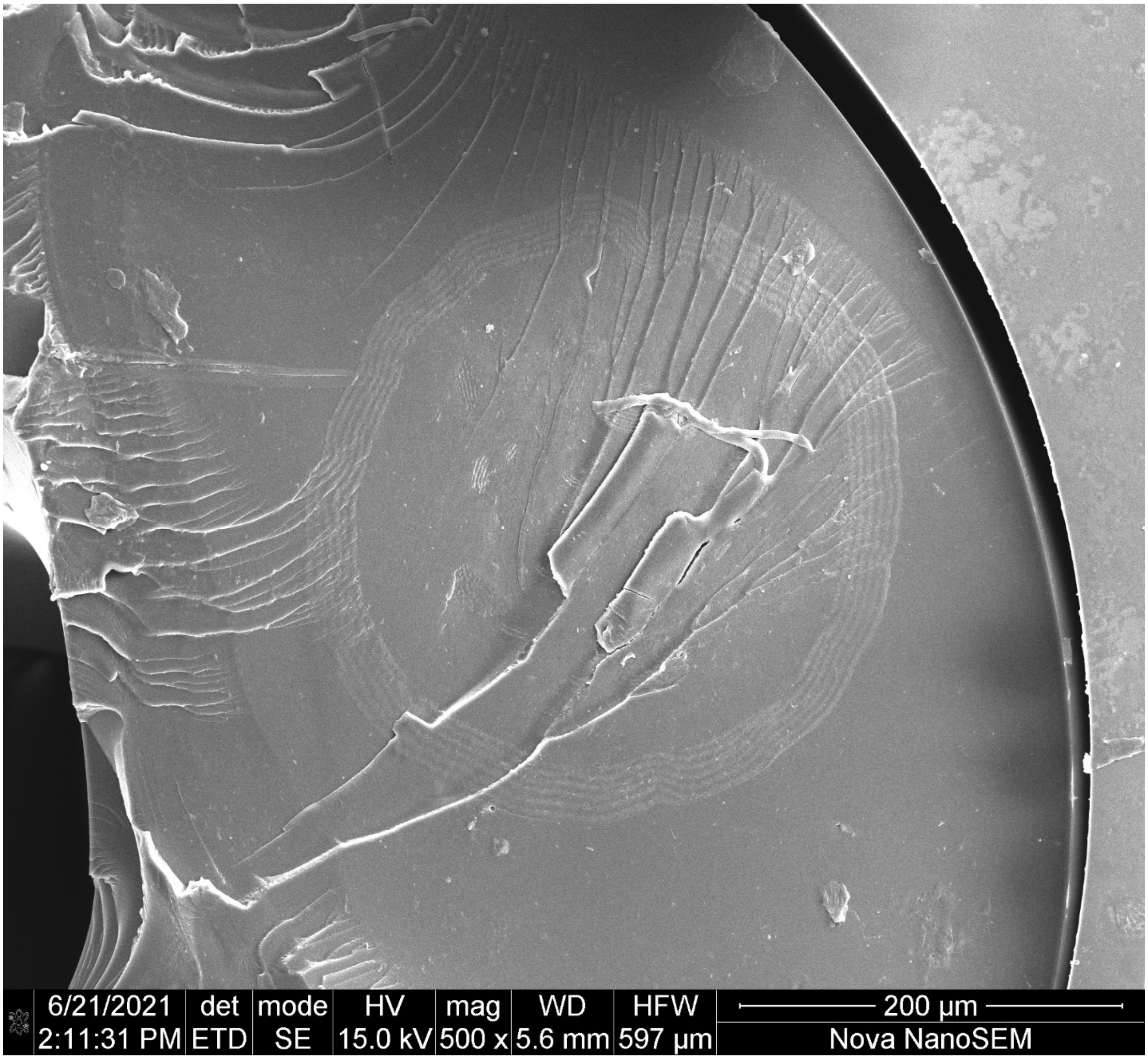

Figure S8. SEM image of cross-section of CNC structure formed inside a capillary tube tilted at 60° and rotated at angular velocity 6.3 s^{-1}. The CNC concentration was 5 wt.%.

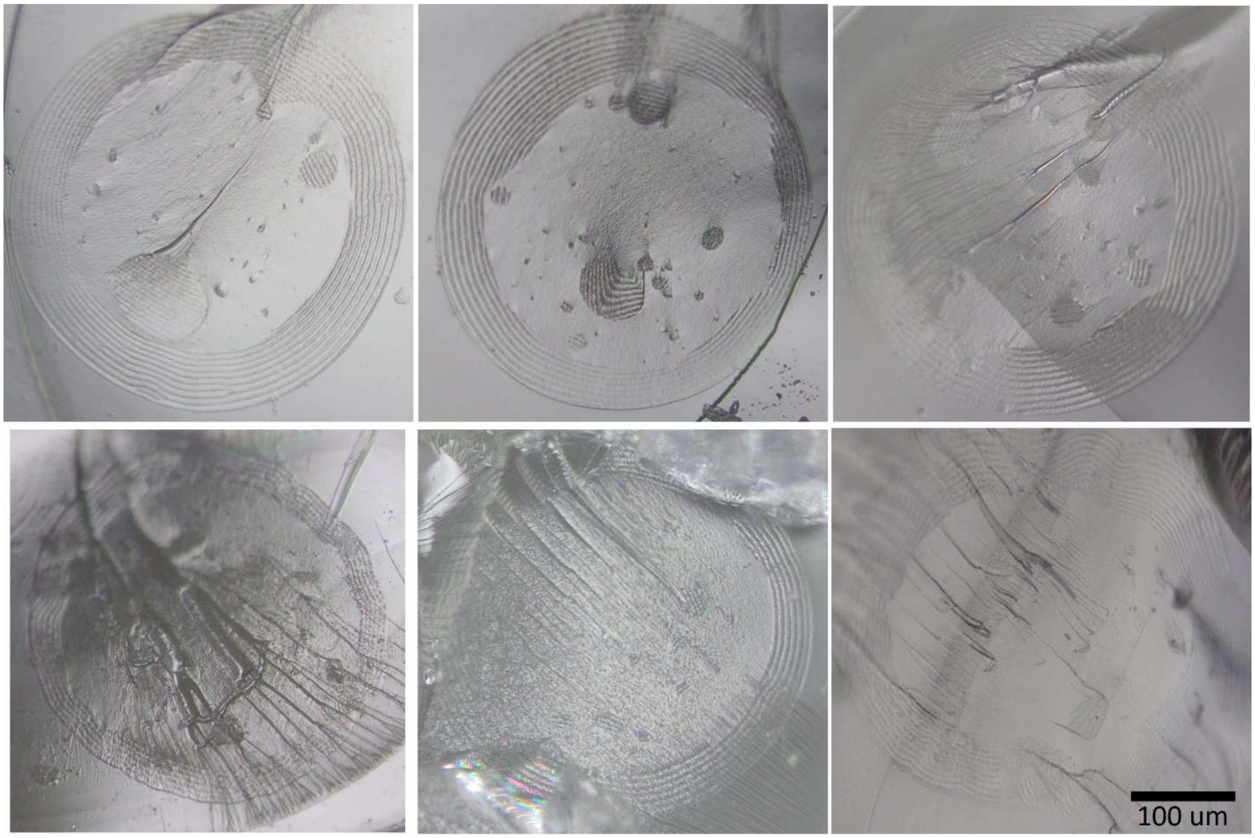

Figure S9. Further cross-section images showing the core-shell structure that forms by tilting and rotating CNC confined inside a capillary tube.